788

On the link between Barents-Kara sea-ice variability and European blocking

P. Ruggieri[1], R. Buizza[2], G. Visconti[1]

Research Department

[1]Department of Physical and Chemical Sciences-CETEMPS, University of L'Aquila, L'Aquila, Italy
[2]ECMWF

Key Points:
-Impact of sea-ice reduction on mid-latitude weather
-Troposphere-Stratosphere interaction

Abstract

This study examines the connection between the variability of sea-ice concentration in the Barents and Kara (B-K) seas and winter European weather on an intra-seasonal time scale. Low sea-ice regimes in autumn and early winter over the B-K seas are shown to affect the strength and position of the polar vortex, and increase the frequency of blocking regimes over the Euro-Atlantic sector in late winter. A hypothesis is presented on the mechanism that links sea-ice over the B-K seas and circulation regimes in the North Atlantic, and is investigated considering 34 years of ECMWF reanalysis data. Four key steps have been identified, starting from a local response of the near-surface fluxes and modification of the upper tropospheric wave-pattern, to the stratospheric adjustment and the tropospheric response in the North Atlantic. The proposed mechanism explains the delayed, late winter response of the North Atlantic Oscillation to the late autumn sea ice reduction, which has been found both in observations and model experiments. It also provides valuable insights on how the reduction of Arctic sea-ice can influence the position of the tropospheric jet in the Euro-Atlantic sector.

1 Introduction

The rapid decline of sea-ice in the Arctic and its potential impact on the extra-tropical circulation have recently instilled great interest in the atmospheric community. In particular, one of the aspects that has attracted attention is whether sea-ice variability over the Barents and Kara (B-K) seas can affect weather conditions over the Euro-Atlantic sector. The investigation and understanding of this link, and in particular the potential impact of B-K sea-ice concentration on blocking regimes in the North Atlantic and temperature anomalies over Europe, is the main topic of this work.

The proposed mechanism that links the two regions is quite complex and, as it will be discussed in this work, it involves two, two-way interactions between the troposphere and the stratosphere, with changes in the tropospheric circulation over the B-K seas leading to variations in the stratospheric flow, which in turn affect the tropospheric flow over the Euro-Atlantic sector. This effect is difficult to disentangle from the local tropospheric response and it is likely to be superimposed on intrinsic variability.

This study is an attempt to provide an organised analysis of this possible interaction mechanism, looking at circulation regimes and troposphere-stratosphere exchange mechanisms linked to the variability of sea-ice. Evidence that tropospheric anomalies can drastically affect the stratosphere is known, and for example was given by *Polvani and Waugh* (2004), who showed that the interaction between the troposphere and the stratosphere on intra-seasonal time scales is actually a two-way coupling rather than a one-way forcing stratosphere-to-troposphere. More recently, *Cohen et al.* (2007) also suggested that the earth surface is one of the primary sources of stratospheric sudden changes, and established a link between surface forcings and the troposphere-stratosphere coupling.

Looking more specifically at the role of the B-K seas, *Kim et al.* (2014) suggested that sea-ice loss in this area in autumn and early winter can cause a weakening of the stratospheric polar vortex in the subsequent months. In other words, it can affect the winter stratospheric circulation. *Cohen et al.* (2013) showed that the observed decline of B-K sea-ice is associated with an increase in Siberian snow cover, and can influence the variability of the stratospheric polar vortex. Other authors, (e.g. *Overland et al.*, 2011; *Francis and Vavrus.*, 2012; *Liu et al.*, 2012; *Tang et al.*, 2013; *Mori et al.*, 2014) have also indicated that autumn and early winter sea-ice anomalies in the B-K seas may cause colder temperatures in mid-latitudes in the following months.

B-K sea-ice anomalies have both a local impact and an influence on the large-scale, upper atmosphere circulation. Locally (i.e. in the proximity of the B-K seas), *Inoue et al.* (2012) and *Kim et al.* (2014) have shown that low ice conditions in the B-K seas are associated with higher sea level pressure in the surroundings of the sea-ice anomaly, a shift of the storm tracks and an increased occurrence of blocking events. Looking at the larger scales, the atmospheric response to this anomalies resembles the negative phase of the Arctic Oscillation, and exhibits a temperature pattern with a canonical Warm Arctic and Cold Continents pattern (*Cohen et al.*, 2013). While the former, local response has been readily attributed to warmer 'Sea Surface Temperatures' and to the presence of larger open water areas, the origin of the latter large-scale response remains, at least partially, uncertain. *Cohen et al.* (2014) has linked this response to an enhanced coupling between the troposphere and the stratosphere, together with other factors characteristic of the 'Warm Arctic Cold Continent' pattern, such as an increase in the Siberian snow cover.

Considering this latter point, *Petoukhov and Semenov* (2010) tested the sensitivity of a general circulation model to the reduction of sea-ice in the B-K seas and found that for the 40%-80% range the response is a negative Arctic Oscillation with a 'Warm Arctic Cold Continent' temperature pattern. They explained that cold anomalies over central Europe, persistent throughout winter, were the tropospheric response to enhanced surface heat fluxes in the B-K seas. *Kim et al.* (2014) argued that the strong heating from the ocean may be responsible for enhanced blocking activity in B-K which is a harbinger for an intense coupling between troposphere and stratosphere.

Going back to the relationship between tropospheric and stratospheric variability, *Woollings et al.* (2008) showed that blocking highs can significantly change the planetary waves in the troposphere causing a vertical propagation into the stratosphere. *Nishii et al.* (2011) provided observational evidences that blocking in the B-K seas region is followed by anomalously high eddy heat fluxes into the stratosphere, and warmer than normal stratospheric temperature up to one month ahead.

The B-K sea-ice variability is statistically linked with the North Atlantic Oscillation (NAO) on intraseasonal time scales, but the dynamical mechanism underlying the link is not well documented in literature. *Yamamoto et al.* (2006) indicated that sea-ice in the Arctic and the NAO are connected. They highlighted that, whereas negative sea-ice cover anomalies in the B-K seas can be induced by a positive NAO in early winter, they tend to cause a negative NAO in late winter. *Strong et al.* (2009) also detected a feedback between the variability of the Arctic sea-ice cover and the NAO, and *Wu and Zhang* (2010) documented an impact of reduced sea-ice anomalies on the large-scale atmospheric circulation over the Euro-Atlantic sector. They made an observational study based on a lagged maximum covariance analysis and found that sea-ice cover anomalies could be used as a predictor for the NAO pattern with a lead time of up to two months. More recently, *Grassi et al.* (2013) tested the sensitivity of the European weather to sea-ice cover reduction and found that it can induce a cooling effect on central and western Europe and more rainy winter conditions in the Mediterranean basin, linked to a negative NAO circulation.

These works suggest that one possible way to investigate the link between autumn B-K sea-ice anomalies and winter surface temperature over Europe is by considering four key steps spanning a 3-4 month period from autumn and early winter (say December-January) to late winter:

1. Autumn and early winter sea-ice concentration anomalies in the B-K seas induce local changes on the tropospheric circulation;

2. Local changes in the tropospheric circulation have an impact on the larger-scale (polar) stratosphere circulation;

3. Changes to the stratospheric circulation and the polar vortex structure influence the large-scale flow over the Euro-Atlantic sector in late winter;

4. Changes in the Euro-Atlantic circulation have tropospheric effects, detectable in particular in the surface temperature over Europe in late winter.

Hereafter, we will discuss how this four-step mechanism can explain the link between B-K sea-ice variability in late autumn/early-winter, and European blocking and surface weather conditions in winter/late-winter. Before we discuss these four steps, in section 2 we present the methodology and the data used in this work. Then, in section 3 the results of our investigation, organized following the four-steps introduced above, are discussed. In section 4 the link between B-K sea-ice and the circulation over the Euro-Atlantic sector is further analysed and few key, open points worth future investigations are outlined. Finally, in section 5 our main results are summarized.

2   Methodology

The atmospheric data used in this study are 2-metre temperature (t2m), geopotential height at all pressure levels, zonal wind at 4 pressure levels (925-850-775-700 hPa), meridional wind and temperature at 100 hPa and potential vorticity (PV) on isentropic levels from the ECMWF Era-Interim reanalysis *Dee et al.* (2011). ERA-Interim covers a period from 1979 to date. These fields have been extracted six-hourly, on a 1-degree, regular, global, latitude/longitude grid. Surface turbulent heat fluxes have been defined as the sum of the surface sensible and latent heat flux. Sea ice concentration is taken form the Hadley Centre Sea Ice and Sea Surface Temperature data set (*Rayner et al.*, 2003). The atmospheric circulation in this sector has been characterized not only in terms of NAO indices, but also in terms of blocking occurrence and low-level jet regimes.

The link between the B-K sea-ice variability and the stratosphere is assessed looking at the eddy heat flux in the lower stratosphere and the polar cap potential vorticity. Winter composites computed for the 9 (of the 34 ERA-Interim years used in this work, 1979-2013) years with the lowest sea-ice (LIYs) and the 9 with highest sea-ice (HIYs) are compared. LIYs and HIYs have been identified by comparing the December sea-ice concentration in an area centered on the B-K seas (30°-70° E, 70°-80° N-the area covered by dots in figure 2a). They are:

- LIYs: 2001, 2004-2009, 2011, 2012;
- HIYs: 1979, 1980, 1981, 1983, 1987, 1988, 1997, 2002, 2003.

Composites of LIYs minus HIYs are analysed through the paper. The NAO pattern has been computed from the first Empirical Orthogonal Function (EOF) of the 500 hPa geopotential height monthly-mean, in the sector 75°W-15°E 20°N-90°N. The EOF of each month is computed taking a three months interval centered on the selected month for the whole 34-year period. The NAO daily index is then obtained by projecting the daily spatial field on the EOF. To classify the regime conditions (blocking in particular) over the Euro-Atlantic sector, a two-dimensional blocking index has been used (following *Tibaldi and Molteni* (1990); TM90 hereafter; see appendix).

To characterize the position of the North Atlantic jet-stream, following Woollings et al. (2010; WO10 hereafter), a Jet Latitude Index (JLI) has been calculated following the same procedure but without removing seasonal cycle (see appendix for its definition). The JLI is a measure of the position of the eddy-driven jet stream in the North Atlantic. It is correlated with blocking in the Euro-Atlantic sector

and its variability can be mostly explained by the combination of the NAO and Eastern Atlantic patterns, as shown in WO10.

3   Results

As indicated in the Introduction, the link between autumn B-K sea-ice anomalies and winter surface temperature over Europe is investigated by discussing the four key steps introduced at the end of Section 1. Figure 1 is a schematic of the four key steps of the propagation of a signal linked to autumn B-K sea-ice anomalies. In early winter the surface fluxes from the ocean heat the troposphere in the surroundings of the B-K seas, and this effect can be associated with blocking in the heating area. A positive geopotential height anomaly over the B-K seas tends to modify the wave pattern at 100 hPa, i.e. to advect warmer-than-average air into the polar cap, leading to a weakening of the stratospheric polar vortex. Then, in late winter, in response to the stratospheric anomaly, a negative Arctic Oscillation pattern emerges as the dominant tropospheric circulation.

3.1   Autumn and early winter B-K sea-ice concentration anomalies, and their local impact on the tropospheric circulation

Figure 2a shows the average difference in sea-ice concentration in the northern Barents sea and the Kara sea between LIYs and HIYs. The sea-ice difference has a peak, on average, in December, with the signal starting being detectable in November and lasting until February. The other panels of figure 2 show the geopotential height difference between LIYs and HIYs at 500 hPa and 30 hPa averaged through the course of winter (DJFM). Although they will be discussed in the following sections, they have been inserted here to summarize, in one figure, the main aspects of the link between the B-K sea-ice concentration and the Euro-Atlantic circulation.

Low ice conditions in the B-K seas are associated with warmer SSTs (not shown, see *Inoue et al.* (2012)): consequently, the atmosphere is subjected to a stronger heating from the ocean. The comparison of the surface fluxes (figure 3) indicates that low ice conditions are associated with a larger area of diabatic heating from the ocean mainly in the sea-ice-free region. In particular, figure 3d shows that a net heating from the ocean is dominant in the area of interest and that the observed anticyclonic anomaly is associated to a particularly strong flux difference in the sea-ice-free area. Although this net heating does not imply that sea ice is a primary forcing of the anticyclonic anomaly , it shows that fluxes due to low sea-ice concentration can have a significant impact. The dipolar pattern found in figure 3c has been associated to the variability of sea-ice also by *Sorokina et al.* (2016); whereas positive anomalies (i.e. the ocean warms the atmosphere) can be readily explained by a change in the surface temperature, we speculate that negative anomalies at lower latitudes can be explained by a feedback from the tropospheric response to low sea-ice or, more generally, by warmer near-surface temperatures associated to low sea-ice.

An interesting question to address is whether the sea-ice difference is the only cause of the changes in the surface heat fluxes, or whether there are other effects, e.g. temperature advection related to blocking, that can also contribute and can possibly cause the reduction of sea-ice, or due to internal variability in general. Figure 4 can help us investigating this point. Panel a) shows the sea ice concentration difference in November-December-January-February (NDJF) with respect to the mean of HIYs + LIYs. The difference is very similar throughout the season with a slightly larger difference in December. This finding suggests that an intraseasonal reduction of sea-ice concentration due to increased blocking activity in the area does not fully explain the observed changes in the surface heat fluxes. The important and possibly dominant role of sea-ice in explaining changes in surface heat fluxes are further confirmed by

comparing the scatter diagrams of surface fluxes in the area enclosed by b) a black line and c) a red line in figure 3c. The values of the Pearson's correlation and Spearman's rank-correlation coefficients suggest that sea ice has a non-negligible feedback on the fluxes in the LIYs-HIYs dataset and the negative pattern observed in figure 3c (which can not be caused directly by sea-ice) is less significant. This is the first key step to link sea-ice variability to the intra-seasonal variability of the atmosphere. The hypothesis of a link between surface turbulent fluxes and anticyclonic circulation regimes in the B-K seas has also been introduced by *Kim et al.* (2014) and investigated by *Mori et al.* (2014).

The atmospheric response to this diabatic source was also discussed by *Petoukhov and Semenov* (2010) and can be detected in the geopotential height at 500 hPa in early winter, as it is shown in Figure 2b, where the dominant pattern is a blocking-like signal over the B-K seas.

Hence, the first hypothetical step implies that the tropospheric response to B-K sea-ice differences is an anticyclonic, blocking-like geopotential anomaly, which can be detected in December and January (see figure 5). This has been discussed by *Deser et al.* (2010), who showed that the atmospheric response to sea-ice reduction is a barotropic positive geopotential height anomaly over Eurasia. Blocking in this region can enhance the vertical propagation of planetary waves, thus the hypothesis that the warming from the ocean can trigger or sustain blocking can potentially extend the link from B-K sea-ice to the stratospheric variability.

3.2   Impact of local changes in the tropospheric circulation on the larger-scale stratosphere circulation

The development of an anticyclonic anomaly over the B-K seas surroundings and over Siberia, and the link with the lower stratospheric circulation has been examined by *Takaya and Nakamura* (2008). A positive geopotential height anomaly in the lower troposphere over the B-K seas in November-December is associated with a modified wave pattern at 100 hPa. This, through a strengthening of a zonally asymmetric temperature dipole, implies a stronger poleward temperature advection by means a zonally asymmetric circulation. This is also an indication of a stronger troposphere-stratosphere interaction. Indeed, *Nishii et al.* (2011), suggest that blocking in B-K is a harbinger of an intensified eddy heat flux up to one month ahead. Also *Kim et al.* (2014) and *Sun et al.* (2015) provide evidence that a reduction of sea ice in B-K is associated with a similar mechanism, and the hypothesis of a precursory blocking signal is consistent with their study.

Following these works, we have assessed the influence of the tropospheric circulation on the stratosphere by looking at the 100 hPa eddy heat flux, a widely used measure of the vertical propagation of planetary waves (see e.g. *Kuroda, Y., and Kodera, K.* , 1999; *Polvani and Waugh*, 2004). The heat flux induces changes in the polar cap potential vorticity (see e.g. *Hinssen and Ambaum*, 2010), as can be seen in figure 6. Following *Hinssen and Ambaum* (2010), we have quantified the link between the lower-stratospheric potential vorticity and the tropospheric heat flux. The sign of the PV in figure 6 has been changed to compared it with the integrated heat flux. The anomalies shown in figure 6 suggest that LIYs are associated to extensive stratospheric potential vorticity anomalies, a fact that indicates a lowering of the intensity of the stratospheric polar vortex in late January and February. The dotted line, computed setting the anomaly to zero in December, suggest that most of the PV anomaly is explained by the heat flux in January with a non-negligible contribution from the heat flux in December.

In other words, the polar vortex is weakened in the lower stratosphere in late January and February by wave activity in December and January, and the increase in the wave activity can be linked with the local response to the heating from the ocean.

These results, supported by *Kim et al.* (2014), can link the variability of sea-ice in the B-K seas to features of the atmospheric circulation modulated by the intensity of the polar vortex.

3.3 Impact of changes to the stratospheric circulation and the polar vortex structure on the large-scale flow over the Euro-Atlantic sector in late winter

Let us now consider the westward and downward propagation of the stratospheric signal into the Euro-Atlantic sector. Much of the variability of the Euro-Atlantic sector, and in particular of the North Atlantic jet stream, is explained by the NAO. Nonetheless, WO10 observed that the variability of the eddy driven North Atlantic jet stream projects both onto the NAO and the Eastern Atlantic pattern. Although there is no exact one-to-one correspondence between a JLI regime and blocking, the trimodality of the probability density function (PDF) of the JLI (see figure 7) can be interpreted in terms of occurrence of blocking in different geographical areas.

Looking at the JLI distributions (figure 7), we can detect one peak at around 35 degrees North, south of the main, central peak. This peak is not present in the HIYs, which compared to the LIYs also show a higher value in the secondary peak at about 55 degrees North. It is worth pointing out that while differences in the LIYs and HIYs distributions are statistically significant at 95% confidence level in correspondence of the third (the southerly) peak at about 35 degrees North, differences are not statistically significant in correspondence of the other two peaks.

As indicated by WO10, the peak at about 35 degrees North is associated to the negative phase of the NAO, and can be used as an indication of the signature of high latitude blocking on the low level jet. WO10 also showed that low JLI values are characteristic of blocking occurring mostly over Greenland and northern Europe. The analysis of the TM90 blocking index shows that LIYs have roughly 5-10% more blocked days than HIYs in the 60W-60E sector, with a peak in the middle of the Atlantic Ocean (not shown). Indications from the 2-dimensional TM90 index (see figure 8) confirm that this signal is related to high-latitude blocking. A similar conclusion can be drawn if the results are compared with *Scherrer et al.* (2006). LIYs and HIYs are associated with distinct blocking regimes in the Atlantic sector, respectively high and low latitude blocking.

As pointed out in the previous subsection, the analysis of the eddy heat flux reveals a weakening of the polar vortex in late January and in February. Hence, the occurrence of high latitude blocking and the meridional regime of the JLI can be linked to feedbacks between the stratosphere and the troposphere. As indicated by *Baldwin and Thompson* (2009), the zonal-mean-EOFs based Northern Annular Mode index (NAM- see appendix for its definition) is a good indicator of stratosphere-troposphere coupling. As shown in figure 9, the difference of the NAM index between LIYs and HIYs confirm the anomalous stratospheric circulation detected in section 3.2 and suggests that the stratophere can have an impact on the tropospheric circulation detected over the North Atlantic sector. Tropospheric feedbacks between the jet and the eddies associated to the downward influence of the lower stratosphere, can explain the anomalous meridional regime of the JLI and the occurence of high latitude blocking. To further elucidate the link between these circulation patterns and the European weather, following the approach used by *Tomassini et al.* (2012), a Regional Geopotential Index is shown in figure 10. It is worth noting that LIYs and HIYs have an opposite signal and their composite shows a persistent difference in mid and late February. This figure indicates that the downward influence is active mostly February when the tropopause pressure difference over the polar cap reaches its maximum and the respective difference over Europe is largely similar.

3.4 Link between changes of the Euro-Atlantic circulation and surface temperature over Europe in late winter

In the previous three sections we have discussed how a B-K sea-ice anomaly can affect firstly the local tropospheric circulation, and then the upper-level stratospheric circulation, eventually changing the loca-

tion and distribution of low-frequency phenomena over the Euro-Atlantic sector. Let us now investigate whether these changes can have an impact also on the low level temperatures over Europe.

The positive and the negative phases of the NAO identify two dominant regimes of the Euro-Atlantic circulation (*Trigo et al.*, 2002), that can be associated with different types of blocking patterns. The European weather response to the alternating phase of the NAO is a dipolar temperature pattern, with cooler temperature in northern Europe during the negative phase. The t2m difference shown in figure 11 can be compared with the results of *Hitchcock and Simpson* (2014), where the impact of the stratosphere on the surface temperature resembles an NAO-like pattern, with strong positive anomalies over the Labrador sea and Greenland and a negative difference over Eurasia, in particular over Scandinavia and Siberia.

In figure 12 the time series of t2m in some areas of the Euro-Atlantic sector are shown. Focusing on the difference between the LIYs and HIYs means, it can be seen that a strong positive signal is detected over Greenland in late winter, a milder signal is found in South-Eastern Europe and a weak negative difference is detected in Scandinavia. It is also worth pointing out that the time series over Scandinavia shows a shift of the difference of the mean between early winter and late winter. The temperature pattern of the LIYs-HIYs difference in the midlatitudes thus project onto the anomalous t2m associated to the downward influence of the stratosphere discussed by *Hitchcock and Simpson* (2014). Instead, it shows positive temperature anomalies over the Arctic, where they find a cooling associated to a downward propagation.

4 Discussion

Four main steps that link sea-ice variability with the European weather have been identified. These steps involve the dynamical interaction between tropospheric and stratospheric features of the atmospheric circulation and can help understanding how sea-ice anomalies determine changes to the thermal forcing of the B-K seas onto the troposphere, and how this projects onto atmospheric modes of variability.

The four-step mechanism introduced in this work provides us with a unified view of how a signal propagates from the B-K seas to Europe. Each step of this mechanism had been already discussed separately in the published literature, and there is not a general agreement on the active role of sea ice, in particular for the impact on mid-latitude weather (e.g. *Gao et al.*, 2015; *Overland*, 2016; *Vihma* , 2014). Our work links them together in a unified mechanism and, although it suffers from large uncertainties (e.g. the shortness of the record and decadal variability embedded in the composite analysis), it establishes a reasonable hypothesis to be tested in further studies. Considering step 1, and in particular the local response to B-K sea-ice concentration anomalies, the atmospheric response to sea-ice reduction in a general circulation model analysed by *Deser et al.* (2010) revealed that both linear and non-linear interactions are involved. More specifically for the case of the B-K seas, *Honda et al.* (2009) argued that near-surface heating caused by sea-ice loss in late autumn (November) can trigger a Rossby wave train in late autumn with anticyclonic anomalies over the Barents sea and cyclonic anomalies over Siberia. Interestingly, they found in late winter a delayed response associated to the negative phase of the NAO (i.e. steps 2 and 3 in our analysis), encouraging further analysis to understand the mechanism responsible for the delay.

Again considering step 1, and now in particular the link between B-K sea-ice and the local circulation, *Mori et al.* (2014) provided robust evidence of the relationship between sea-ice loss and atmospheric blocking high in the Siberian seas. They conjecture that blocking is favored by a slower zonal flow caused by a weakened surface meridional temperature gradient.

Moving to step 2, *Nishii et al.* (2011) showed that blocking in the B-K seas precedes intense upward propagation of planetary waves with a lag of a couple of weeks and is followed by anomalously high stratospheric temperature up to one month ahead.

In figure 6, the northward eddy heat flux at 100 hPa in December and January could be explained by the

intensified blocking activity detected in figure 4. Subsequently, the heat flux can be linked to the stratospheric anomaly, i.e. a weak polar vortex, up to the end of February. The latter mechanism was analysed by *Takaya and Nakamura* (2008). They showed how an external Rossby wave train in the troposphere, with an anticyclonic anomaly over the B-K seas, can potentially change the climatological temperature and geopotential height fields in the lower stratosphere, leading to advection of warm air into the stratospheric polar cap and to a weakening of the polar vortex. In their analysis, a tropospheric wave train in November is associated to a surface Arctic Oscillation signal in January.

The hypothesis of enhanced blocking activity due to anomalous heating from the surface was also introduced by *Kim et al.* (2014) to link sea-ice variability with the intensity of the stratospheric polar vortex, with the same mechanism discussed in sections 3.1 and 3.2. A similar mechanism has been introduced by *Cohen et al.* (2007) to link the Eurasian snow cover in Autumn to the surface Arctic Oscillation in late winter. The idea that an anomaly of potential vorticity near the surface can reach the lower stratosphere and then be transmitted to the troposphere again was exploited by *Ambaum and Hoskins* (2002) to explain the long-term (15-20 days) autocorrelation of the NAO index. The cross-section of the geopotential height difference in the North Atlantic and the map of the tropopause height difference in figure 13 suggest that the same mechanism can be relevant in the analysis presented in this study. Considering the dynamical link between stratospheric anomalies and tropospheric anticyclonic anomalies, a feedback between blocking and the polar vortex may be responsible for the increased occurrence of the negative NAO in late winter for the LIYs case (figure 13c). The conjecture is that the downward propagation of B-K sea-ice related stratospheric anomalies on a time scale of few weeks can favor the occurrence of high latitude blocking in the North Atlantic.

A different view of the link can attribute a central role to the dynamics of the jet-stream and its impact on the occurrence of blocking over the North Atlantic. The zonal wind response to stratospheric forcings has been analysed by many studies (e.g. *Kushner, P. J., and Polvani, L. M.* , 1999; *Haigh et al.*, 2013; *Simpson et al.*, 2009). Interestingly, in our results the equatorward shift of the low-level jet in the LIYs-HIYs difference can only be detected over the Atlantic Ocean (not shown). A negative NAO, associated to blocking, in February and March, could be intepreted as the zonally asymmetric response of the troposphere to anomalies in the lower stratosphere.

Finally, considering step 4, the impact on the European weather slightly differs from the canonical pattern of the NAO, but still projects onto the NAO (see also *Budikova* (2009)). Thus, at first glance, the implications of the mechanism in figure 1 on the temperature over Europe can be described in terms of a synoptic response to the regime of the NAO associated to blocking in the North Atlantic. Nevertheless, the t2m difference observed in figure 11 does not match the one commonly associated with the negative NAO (e.g. *Trigo et al.*, 2002). The t2m difference over the Euro-Atlantic sector, discussed in sections 3.4, can be mostly explained by the occurence of blocking and a shift of the jet, and the analysis carried out in the previous sections suggest that the role of the stratosphere is unlikely to be negligible.

5 Conclusion

In this study, the link between sea-ice variability in the Barents and Kara seas and the European weather has been analysed and explained by a 4-step mechanism involving two, two-way troposphere-stratosphere interactions. Low ice regimes in late autumn and early winter (say December-January) have been associated to a high latitude blocking regime in the North Atlantic in late winter (say February-March).

The role of sea-ice in the mechanism is related to the influence it has on the above troposphere, specifically to the non-linear local response in terms of blocking.

The atmospheric connections between blocking in the Barents-Kara seas region, the stratospheric cir-

culation and the weather in the Euro-Atlantic sector have been described by a modification of the wave pattern at 100 hPa and by the stratospheric feedback on blocking. The evidence of the link, also supported by other studies, relies on the key assumption that low sea-ice conditions lead to more blocking in Barents-Kara via turbulent surface fluxes. The results of this study support the hypothesis that the reduction of Arctic sea-ice concentration can lead to more high latitude blocking events and a slower tropospheric jet.

A   Appendix

In this appendix some indices and methods used in the previous sections are described:

1. The TM90 blocking index

2. The heat flux-PV relation

3. The Jet Latitude Index (JLI)

4. The Regional Geopotential Index and The Northern Annular Mode index

The statistical tests used in the work are also briefly described in sub-section A5.

A.1   The TM90 blocking index

The TM90 index introduced in the paper has been computed as follows: the geopotential height at 500 hPa daily field is filtered with a 5 days running mean and the gradients are calculated at every latitude:

$$GHGS = \quad \frac{Z(\phi_0) - Z(\phi_s)}{(\phi_0 - \phi_s)} \tag{1}$$

$$GHGN = \quad \frac{Z(\phi_n) - Z(\phi_0)}{(\phi_n - \phi_0)} \tag{2}$$

where

$$\phi_n = \quad \phi + \Delta\phi \tag{3}$$

$$\phi_0 = \quad \phi \tag{4}$$

$$\phi_s = \quad \phi - \Delta\phi \tag{5}$$

the increment $\Delta\phi$ is taken as $15°$, which is needed to compute the index up to $75°$ N, and the results are not sensitive to this choice. The parameter Δ, introduced in the original paper to compute the index around a fixed latitude, i.e. $\Delta = 0, \pm 4$, is now fixed to 0 and the thresholds for the gradients are left unchanged (i.e. 0 m/deglat for GHGS and -10 m/deglat for GHGN). No criteria for temporal persistence and spatial coherency have been applied.

A.2　The heat flux-PV relation

The integration of the 100 hPa eddy heat flux in figure 7 is based on *Hinssen and Ambaum* (2010). The polar cap potential vorticity difference is obtained from the 100 hPa eddy heat flux difference following:

$$\Delta\langle q\rangle(t) = A \int_0^t \Delta F(t-t')e^{-t'/\tau}dt', \tag{6}$$

where the angular brakets denote the average northward of 60°N, F(t) is the 100 hPa eddy heat flux, τ and A are phaenomenological parameters taken from the climatology, particularly:

$$\tau = -50ln(\theta) + 375 \tag{7}$$

where θ is the potential temperature. The integration starts from the first of November. The 100 hPa eddy heat flux is $[v^*T^*]$ where the square brackets denote the zonal mean and the asterisk denotes the deviation from the zonal mean, v is the meridional component of the wind, T is the temperature. The flux F is obtained from the area-weighted average between 40° N and 80° N of the zonal mean $[v^*T^*]$. The polar cap average PV is obtained as the area-weighted average of the PV northward of 60° N.

A.3　The Jet Latitude Index

The Jet Latitude Index is obtained, as in WO10, from the zonal wind, with the following steps:

1. The daily mean zonal wind is averaged over 4 pressure levels (925-850-775-700 hPa).

2. The field is averaged between 60°W-0°E in the latitudinal band 15°N-75°N.

3. The resulting field is filtered with a 10 day Lanczos filter.

4. The maximum of the filtered field is identified and the JLI is defined as the corresponding latitude.

Three peaks of the distribution are found as in WO10; the trimodality of the PDF is preserved in the LIYs + HIYs ensemble but is lost in one of the 9 years subset. Anyway, the conservation of the properties of each regime in the subsets has been tested. If the latitude of the three peaks of the PDF is taken from the LIYs + HIYs and then 121 days around that latitude are taken for the subset of LIYs and HIYs, then the vertical cross sections of the zonal wind and the horizontal geopotential height at 500 hPa fields are quantitatively in agreement with those in WO10 (not shown).

A.4　The Regional Geopotential Index and the Northern Annular Mode index

The Regional Geopotential Index is computed following *Tomassini et al.* (2012) and it measures the difference between the geopotential height in the area 30W-90E 65N-80N and in the area 0E-40E 45N-55N. The average of these field is taken instead of the maximum. As indicated in *Tomassini et al.* (2012), it is a good measure of a synoptic pattern associated to cold spells over Europe.

The NAM index is defined following *Baldwin and Thompson* (2009), using the Zonal-Mean EOFs method. The EOF is obtained from the zonally averaged geopotential height in the northern hemisphere at each pressure level between 850 and 1 hPa.

A.5   Statistical methods

The PDFs in the paper are estimated with the kernel method of *Silverman* (1981). Statistical significance for the composites has been tested with a two-tailed Students t-test, while for the JLI PDFs a bootstrap method has been applied: for each winter (DJFM) from 1979-80 to 2013-14 the JLI is computed, then two subsets of 9 years each are randomly selected and two PDFs are generated. The distribution of the punctual difference between a couple of PDFs is computed for each latitude. If the difference between the smooth PDFs exceed the 95th percentile of the distribution then it is considered statistically significant. Further details about the statistical tests used in this study can be found in *Wilks* (2011).

Acknowledgments

References

Ambaum, M. H., and Hoskins, B. J. (2002), The NAO troposphere-stratosphere connection, *Journal of Climate*, *15*(14), 1969–1978, doi: http://dx.doi.org/10.1175/1520-0442(2002)015⟨1969:TNTSC⟩2.0.CO;2.

Baldwin, M. P. and Thompson, D. W.J. (2009), A critical comparison of stratospheretroposphere coupling indices., *Q.J.R. Meteorol. Soc.*, *135*, 16611672, doi: 10.1002/qj.479.

Budikova, D. (2009), Role of Arctic sea ice in global atmospheric circulation: A review, *Global and Planetary Change*, *68*(3), 149-163.

Cohen, Judah, et al.(2007), Stratosphere-troposphere coupling and links with Eurasian land surface variability., *Journal of Climate*, *20*(21), 5335-5343, doi: 10.1175/2007JCLI1725.1.

Cohen, J., J. Jones, J.C. Furtado, and E. Tziperman. (2013), Warm Arctic, cold continents: A common pattern related to Arctic sea ice melt, snow advance, and extreme winter weather, *Oceanography*, *26*(4), 150–160, http://dx.doi.org/10.5670/oceanog.2013.70

Cohen, Judah, et al. (2014), Recent Arctic amplification and extreme mid-latitude weather, *Nature geoscience*, *7*(9), 627–637, doi: 10.1038/ngeo2234.

Dee, D. P., Uppala, S. M., Simmons, A. J., Berrisford, P., Poli, P., Kobayashi, S., Andrae, U., Balmaseda, M. A., Balsamo, G., Bauer, P., Bechtold, P., Beljaars, A. C. M., van de Berg, L., Bidlot, J., Bormann, N., Delsol, C., Dragani, R., Fuentes, M., Geer, A. J., Haimberger, L., Healy, S. B., Hersbach, H., Hlm, E. V., Isaksen, L., Kllberg, P., Khler, M., Matricardi, M., McNally, A. P., Monge-Sanz, B. M., Morcrette, J.-J., Park, B.-K., Peubey, C., de Rosnay, P., Tavolato, C., Thpaut, J.-N. and Vitart, F. (2011), The ERA-Interim reanalysis: configuration and performance of the data assimilation system, *Q.J.R. Meteorol. Soc*, 137: 553–597, doi: 10.1002/qj.828.

Deser, C., Tomas, R., Alexander, M., and Lawrence, D. (2010), The seasonal atmospheric response to projected Arctic sea ice loss in the late twenty-first century, *Journal of Cliamte*, *23*(2), 333–351, doi: 10.1175/2009JCLI3053.1. .

Francis, J. A., and Vavrus, S. J. (2012), Evidence linking Arctic amplification to extreme weather in midlatitudes, *Geophysical Research Letters*, *39*(6), doi: 10.1029/2012GL051000.

GAO, Yongqi, et al (2015), Arctic sea ice and Eurasian climate: A review. , *Advances in Atmospheric Sciences*, *32*(1), 92-114.

Grassi, B., Redaelli, G., and Visconti, G. (2013), Arctic sea ice reduction and extreme climate events over the Mediterranean region, *Journal of Climate*, *26*(24), 10101–10110, doi: 10.1175/JCLI-D-12-00697.1.

J. D. Haigh, M. Blackburn, and R.Day (2005), The Response of Tropospheric Circulation to Perturbations in Lower-Stratospheric Temperature., *Journal of Climate*, *18*(17), 3672-3685.

Hinssen, Y. B., and Ambaum, M. H. (2010), Relation between the 100-hPa heat flux and stratospheric potential vorticity, *Journal of the Atmospheric Sciences*, *67*(12), 4017–4027, doi: 10.1175/2010JAS3569.1.

Hitchcock, Peter, and Isla R. Simpson (2014), The Downward Influence of Stratospheric Sudden Warmings, *Journal of the Atmospheric Sciences*, *71*(10), 3856–3876.

Honda, M., Inoue, J., and Yamane, S. (2009), Influence of low Arctic seaice minima on anomalously cold Eurasian winters, *Geophysical Research Letters*, *36*(8), doi: 10.1029/2008GL037079.

Inoue, J., Hori, M. E., and Takaya, K. (2012), The role of Barents Sea ice in the wintertime cyclone track and emergence of a warm-Arctic cold-Siberian anomaly, *Journal of Climate*, *25*(7), 2561–2568, doi: 10.1175/JCLI-D-11-00449.1.

Kim et al. (2014), Weakening of the stratospheric polar vortex by Arctic sea-ice loss, *Nature communication*, *5*, doi: 10.1038/ncomms5646.

Kuroda, Y., and Kodera, K. (1999), Role of planetary waves in the stratosphere-troposphere coupled variability in the northern hemisphere winter, *Geophysical Research Letters*, *26*(15), 2375–2378, doi: 10.1029/1999GL900507.

Kuroda, Y., and Kodera, K. (2004), Stratosphere-troposphere coupling in a relatively simple AGCM: The role of eddies., *Journal of climate*, *17*(3), 629-639.

Liu, J., Curry, J. A., Wang, H., Song, M., and Horton, R. M. (2012), Impact of declining Arctic sea ice on winter snowfall, *Proceedings of the National Academy of Sciences*, *109*(11), 4074–4079, doi: 10.1073/pnas.1114910109.

Mori, M., Watanabe, M., Shiogama, H., Inoue, J., and Kimoto, M.(2014), Robust Arctic sea-ice influence on the frequent Eurasian cold winters in past decades, *Nature Geoscience*, doi: 10.1038/ngeo2277.

Overland, J. E., Wood, K. R., and Wang, M(2011), Warm Arctic-cold continents: climate impacts of the newly open Arctic Sea *Polar Research*, *30*, doi: 10.3402/polar.v30i0.15787.

Overland, J. E. , (2016), Is the melting Arctic changing midlatitude weather? *Physics Today*, *69*(3), 38; doi: 10.1063/PT.3.3107.

Nishii, K., Nakamura, H., and Orsolini, Y. J. (2011), Geographical dependence observed in blocking high influence on the stratospheric variability through enhancement and suppression of upward planetary-wave propagation, *Journal of Climate*, *24*(24), 6408–6423, doi: http://dx.doi.org/10.1175/JCLI-D-10-05021.1.

Petoukhov, V., and Semenov, V. A. (2010), A link between reduced BarentsKara sea ice and cold winter extremes over northern continents, *Journal of Geophysical Research: Atmospheres (19842012)*, *115*(D21), doi: 10.1029/2009JD013568.

Polvani, L. M., and Waugh, D. W. (2004), Upward wave activity flux as a precursor to extreme stratospheric events and subsequent anomalous surface weather regimes, *Journal of climate*, *17*(18), 3548–3554, doi: http://dx.doi.org/10.1175/1520-0442(2004)017¡3548:UWAFAA¿2.0.CO;2.

Rayner, N. A., et al. (2003), Global analyses of sea surface temperature, sea ice, and night marine air temperature since the late nineteenth century, *Journal of Geophysical Research: Atmospheres (1984-2012)*, *108*(D14), doi: 10.1029/2002JD002670.

Scherrer, S. C., CrociMaspoli, M., Schwierz, C., and Appenzeller, C. (2006), Two-dimensional indices of atmospheric blocking and their statistical relationship with winter climate patterns in the Euro-Atlantic region, *International journal of climatology*, *26*(2), 233–249, doi: 10.1002/joc.1250.

Silverman, B. W. (1991), Using kernel density estimates to investigate multimodality, *Journal of the Royal Statistical Society. Series B (Methodological)*, 97–99.

Simpson, I. R., Blackburn, M., and Haigh, J. D. (2009), The role of eddies in driving the tropospheric response to stratospheric heating perturbations., *Journal of the Atmospheric Sciences*, 66(5), 1347-1365.

Song, Y., and Robinson, W. A. (2004), Dynamical mechanisms for stratospheric influences on the troposphere, *Journal of the atmospheric sciences*, *61*(14), 1711–1725, doi: http://dx.doi.org/10.1175/1520-0469(2004)061⟨1711:DMFSIO⟩2.0.CO;2.

Sorokina, S. A., Li, C., Wettstein, J. J., and Kvamst, N. G. (2016), Observed Atmospheric Coupling between Barents Sea Ice and the Warm-Arctic Cold-Siberian Anomaly Pattern, *Journal of Climate*, *29*(2), 495-511.

Strong, C., Magnusdottir, G., and Stern, H. (2009), Observed feedback between winter sea ice and the North Atlantic Oscillation, *Journal of Climate*, *22*(22) 6021–6032, doi: http://dx.doi.org/10.1175/2009JCLI3100.1.

Sun, L., Deser, C., and Tomas, R. A. (2015), Mechanisms of Stratospheric and Tropospheric Circulation Response to Projected Arctic Sea Ice Loss, *Journal of Climate*, *28*(19), 7824-7845.

Takaya and Nakamura (2008), Precursory changes in planetary wave activity for midwinter surface pressure anomalies over the Arctic , *Journal of the Meteorological Society of Japan*, *86*(3), 415–427, doi: http://doi.org/10.2151/jmsj.86.415.

Tang, Q., Zhang, X., Yang, X., and Francis, J. A. (2013), Cold winter extremes in northern continents linked to Arctic sea ice loss, *Environmental research letters*, *8*(1), 014036, doi: 10.1088/1748-9326/8/1/014036

Tibaldi, S. and Molteni, F. (1990), On the operational predictability of blocking, *Tellus A*, 42:343–365, doi:http://dx.doi.org/10.3402/tellusa.v42i3.11882.

Tomassini, L., Gerber, E. P., Baldwin, M. P., Bunzel, F., and Giorgetta, M. (2012), The role of stratosphere-troposphere coupling in the occurrence of extreme winter cold spells over northern Europe, *Journal of Advances in Modeling Earth Systems*, *4*(4), doi: 10.1029/2012MS000177.

Trigo, Ricardo M., Timothy J. Osborn, and Joo M. Corte-Real.(2002), The North Atlantic Oscillation influence on Europe: climate impacts and associated physical mechanisms, *Climate Research*, *20*(1), 9–17.

Trigo, R. M., Trigo, I. F., DaCamara, C. C., and Osborn, T. J. (2004), Climate impact of the European winter blocking episodes from the NCEP/NCAR reanalyses, *Climate Dynamics*, *23*(1), 17–28, doi: 10.1007/s00382-004-0410-4.

Vihma, T. (2014),Effects of Arctic sea ice decline on weather and climate: a review, *Surveys in Geophysics,*, *35*(5) ,1175-1214

Wilks, D. S. (2011), Statistical methods in the atmospheric sciences, *Academic Press*, (Vol. 100)

Woollings, T., Hoskins, B., Blackburn, M., and Berrisford, P. (2008), A New Rossby Wave-Breaking Interpretation of the North Atlantic Oscillation, *Journal of the Atmospheric Sciences*, *65*(2), 609–626, doi: 10.1175/2007JAS2347.1

Woollings, T., Hannachi, A., and Hoskins, B. (2010), Variability of the North Atlantic eddy-driven jet stream, *Quarterly Journal of the Royal Meteorological Society*, *136*(649), 856–868, doi: 10.1002/qj.625

Wu, Q., and Zhang, X. (2010), Observed forcing-feedback processes between Northern Hemisphere atmospheric circulation and Arctic sea ice coverage, *Journal of Geophysical Research: Atmospheres (1984-2012)*, *115*(D14), doi: 10.1029/2009JD013574.

Yamamoto, K., Tachibana, Y., Honda, M., and Ukita, J.(2006), Intra-seasonal relationship between the Northern Hemisphere sea ice variability and the North Atlantic Oscillation, *Geophysical research letters*, *33*(14), doi: 10.1029/2006GL026286.
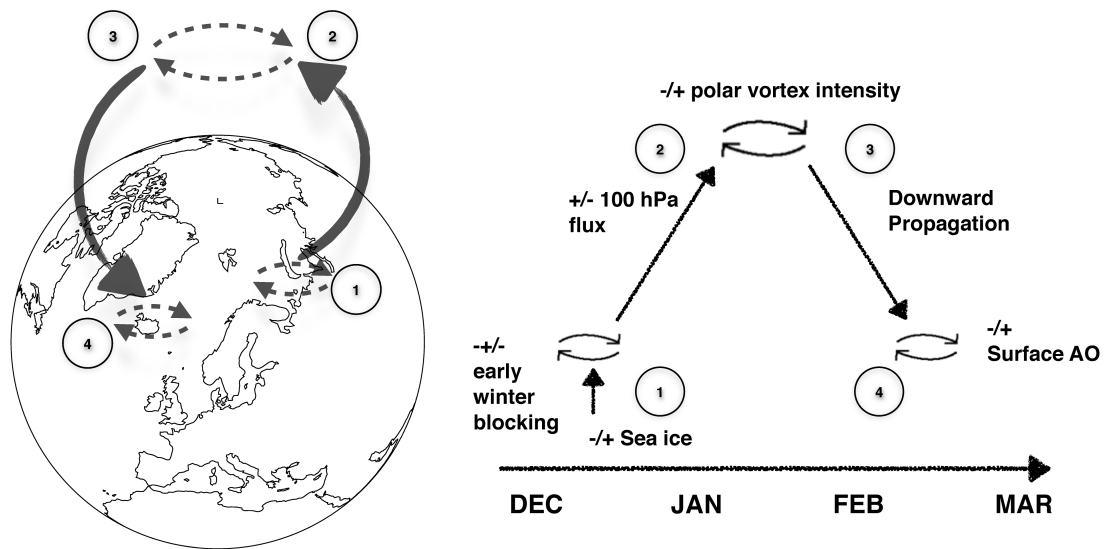
Figure 1: Schematic of the troposphere-stratosphere coupling linking late autumn B-K sea-ice variability to late winter Euro-Atlantic conditions: 1) Autumn and early winter negative (positive) sea-ice anomalies lead to more (less) blocking in the B-K seas. 2) The occurrence of more (less) blocking in the B-K seas is linked to enhanced (reduced) upward propagation of planetary waves into the stratosphere causing a weakening (strengthening) of the polar vortex. 3) The downward propagation of the signal brings to 4) surface anomalies resembling the negative (positive) phase of the Arctic Oscillation with an impact on European near-surface temperatures .

a) SIC LIYs minus HIYs DEC-JAN
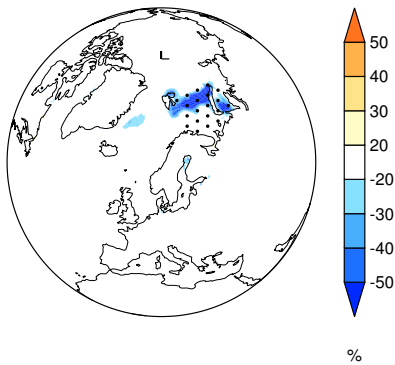
b) z500 LIYs minus HIYs DEC-JAN
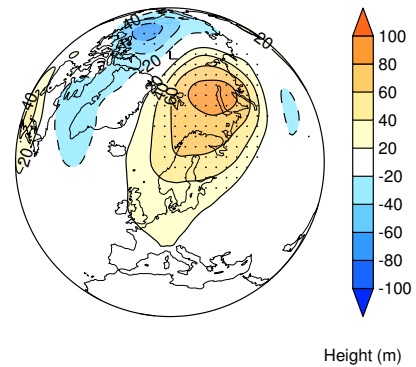
c) z30 LIYs minus HIYs JAN-FEB
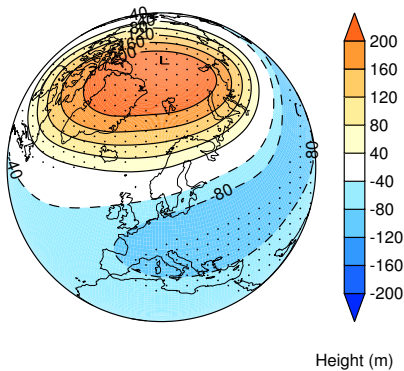
d) z500 LIYs minus HIYs FEB-MAR
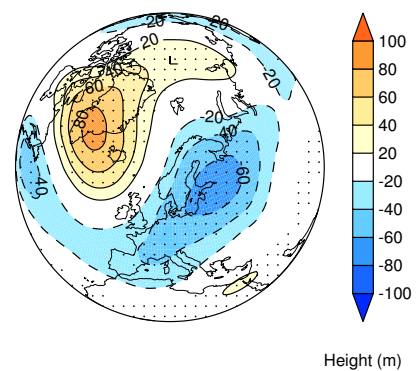
Figure 2: a) Sea-ice concentration (%) difference for LIYs minus HIYs. Dots cover the area used to define LIYs and HIYs. b) 500 hPa geopotential height difference (m) for LIYs minus HIYs in December and January; an anticyclonic anomaly is detected over the B-K seas and over Scandinavia. c) As in b, but at 30 hPa for January and February; a positive geopotential height difference over the polar cap indicates a weak polar vortex. d) As in b, but for February and March; the dipole anomaly projects onto the negative phase of the NAO and strongly resembles the pattern associated to the southern jet regime of the JLI (see section 2 and the appendix for the definition of the JLI. Dots indicate values exceeding 95% confidence level.
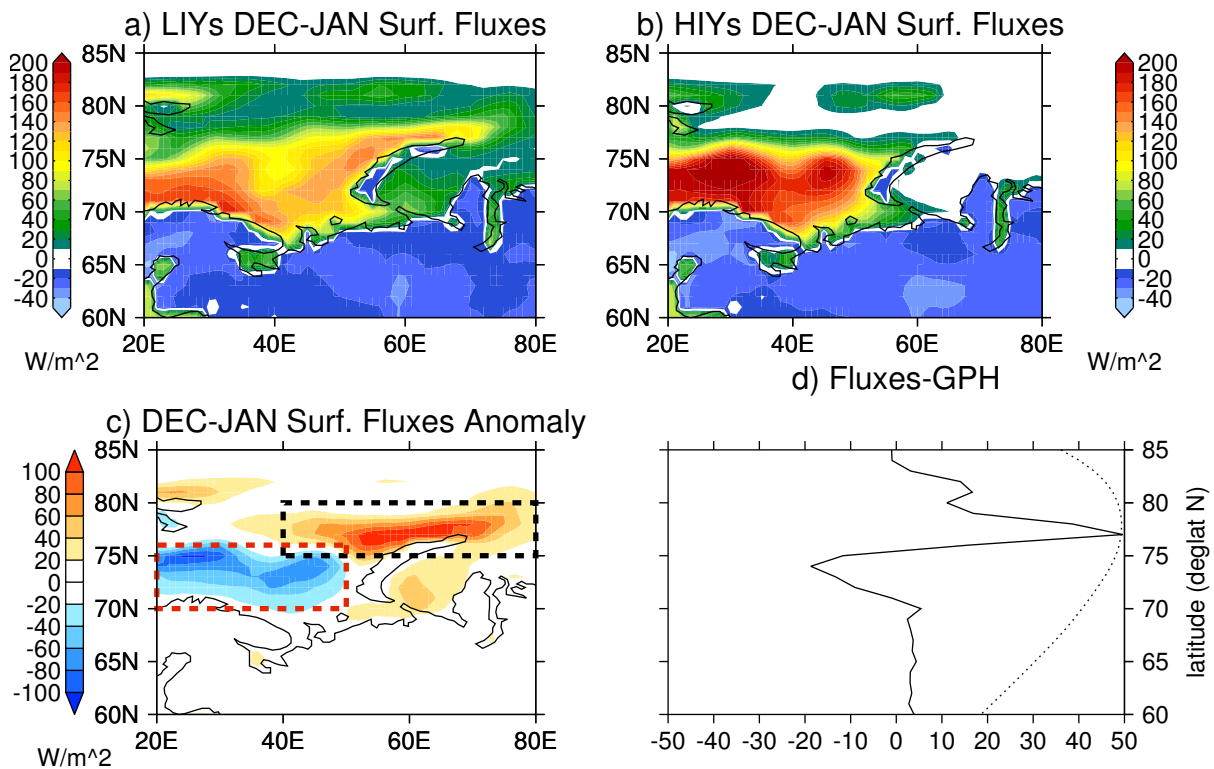
Figure 3: a) Surface turbulent fluxes W/m² in December and January for LIYs and b) HIYs. c) Difference in surface turbulent fluxes (LIYs minus HIYs). d) Difference in surface turbulent fluxes anomaly (LIYs minus HIYs - solid line) and corresponding 500 hPa geopotential height (dotted line, arbitrarily rescaled) averaged over the sector 20°E-80°E .
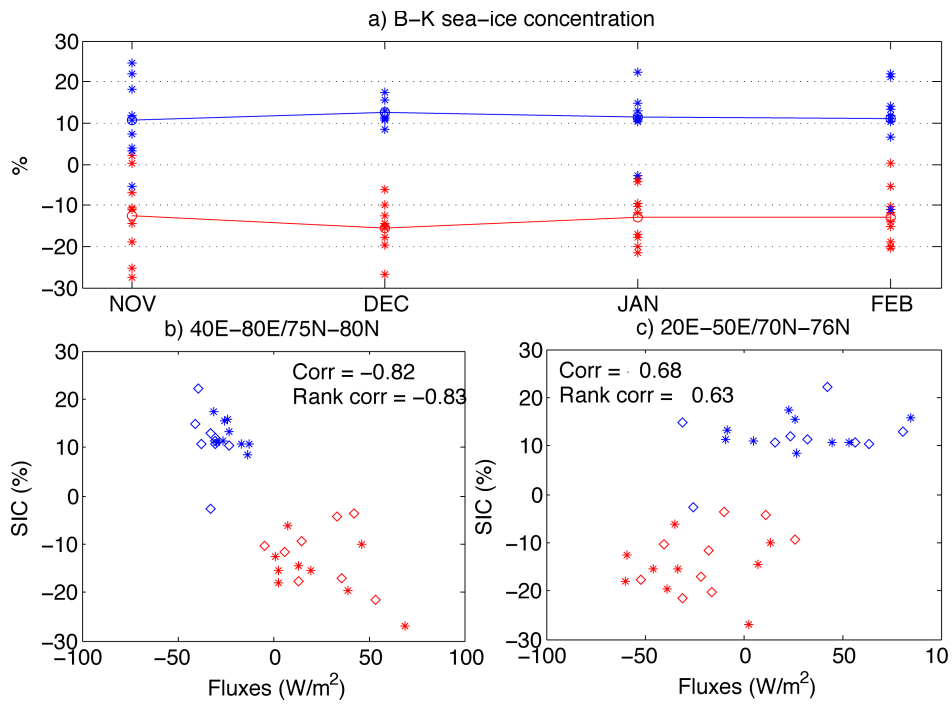
Figure 4: a) Monthly sea ice concentration (%) for HIYs (blue) and LIYs (red) with respect to the mean of the HIYs+LIYs ensemble. b) Scatter plot of sea ice concentration and surface fluxes anomaly in the area enclosed by the black dashed line in figure 3c, with squares for January and asterisks for December. The Pearson's correlation coefficient and the Spearman rank-correlation coefficient between the sea-ice anomaly and the flux anomaly are also reported. As in b) but for the area enclosed by the red dashed line.

a)

LIYs 2DTM90 Index-75N

HIYs 2DTM90 Index-75N

b)

LIYs 2DTM90 Index-65N

HIYs 2DTM90 Index-65N

Number of events

Number of events
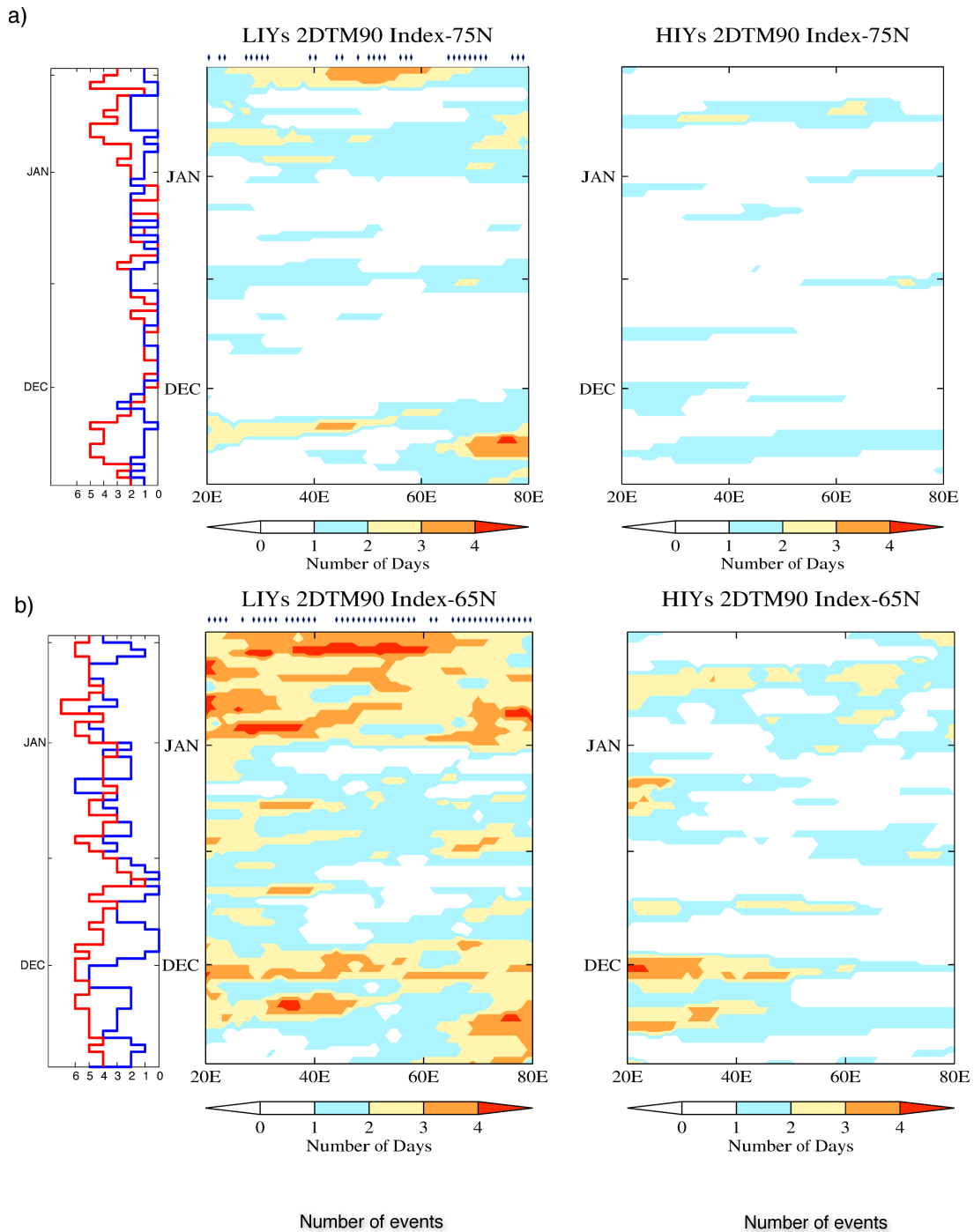
Figure 5: a) The time series of the number of years that have a blocked longitude in the sector 20°E-80°E at 75° N, the red line for LIYs and the blue line for HIYs (left). Hövmoller diagrams of the blocking index based on Tibaldi and Molteni (1990) for LIYs (middle) and HIYs (right) at 75° N over the Barents-Kara region. The index counts the number of times the latitude is blocked at a certain logitude on a specific day of the year. More blocking events are detected in the LIYs in early winter, as stated in section 3.1. b) As in a) but for 65°N. The diamonds mark longitudes where the difference is statistically significant at 95% confidence level according to a two-sample bootstrap test.

a) Polar Cap PV 60N-90N

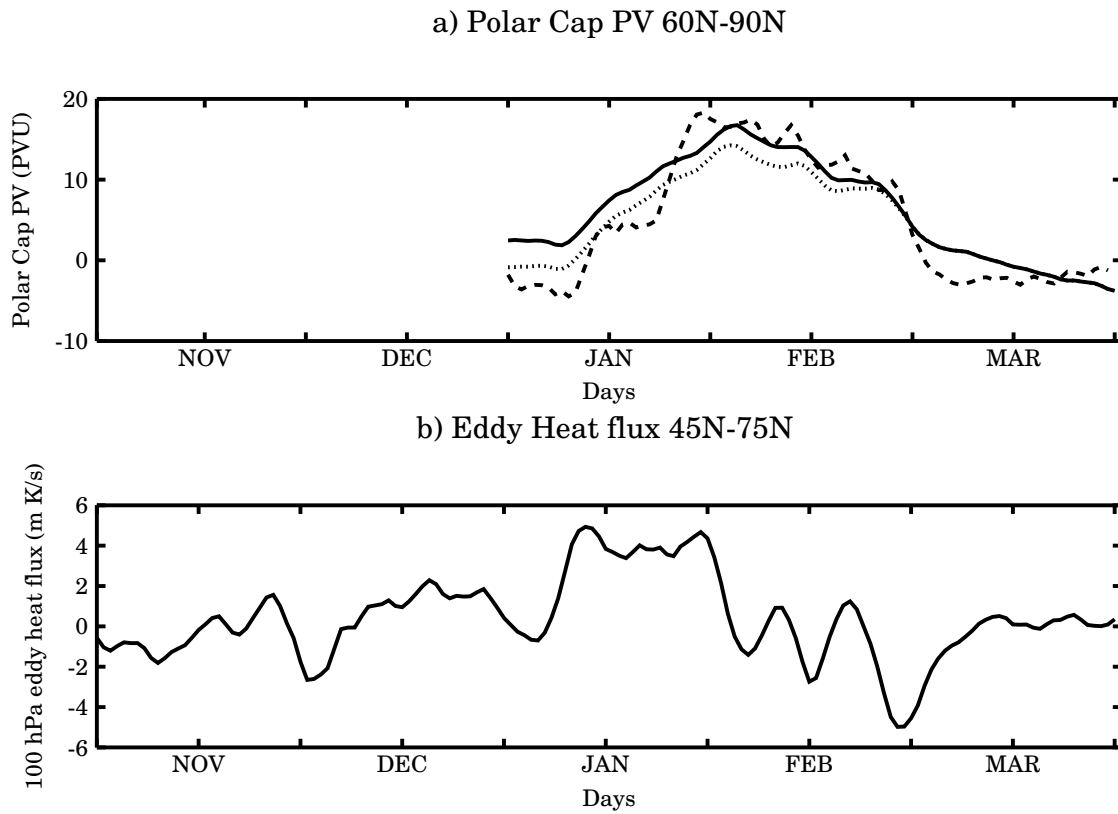
b) Eddy Heat flux 45N-75N

Figure 6: a) Polar cap PV difference (PVU) for LIYs minus HIYs from reanalysis (dashed line, note that sign has been inverted) and predicted from the 100 hPa eddy heat flux with the methodology described in the appendix (solid line). The PV difference in the second half of January and in February is explained by the high poleward heat flux in the lower stratosphere. See section 3.2 for further details. The dotted line is the heat flux integrated setting the anomaly to zero December. b) Five day running mean of the 100 hPa eddy heat flux difference (m·K/s). Positive peaks are found in December and January.

Jet Latitude Index-DJFM
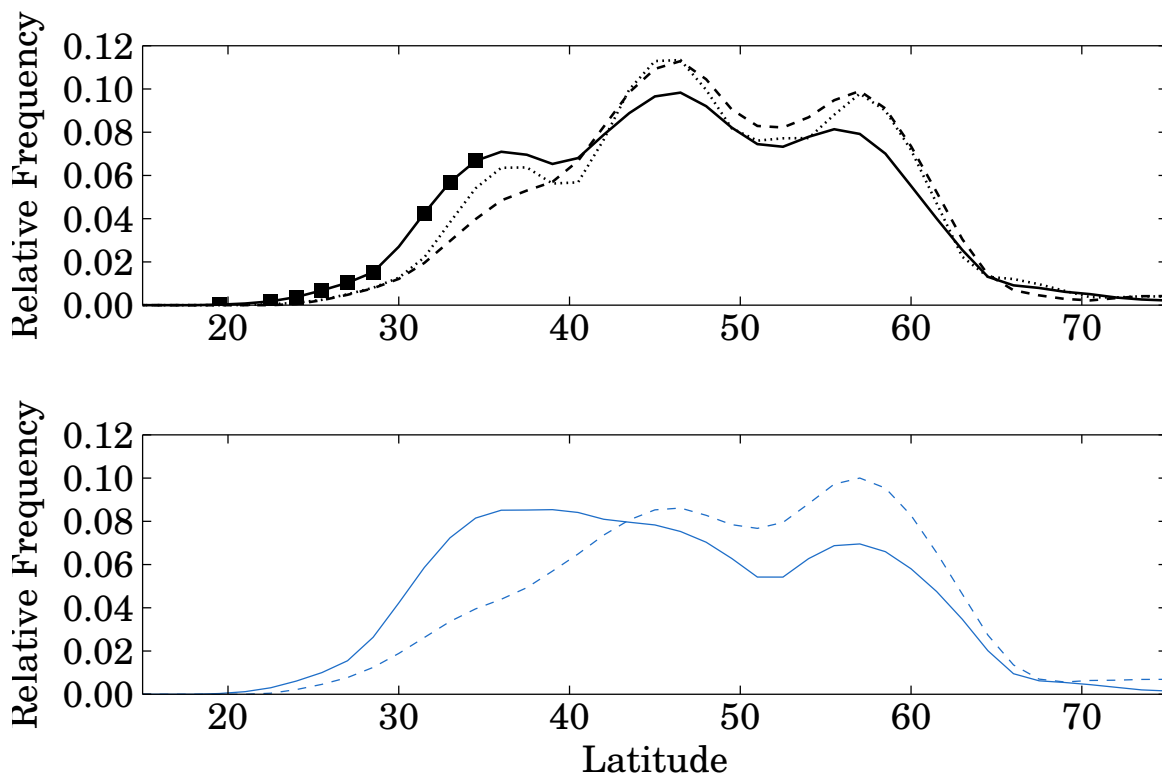
Figure 7: top) PDFs of the Jet latitude index in DJFM for the LIYs (solid line), the HIYs (dashed line) and Era-Interim (dotted line). The units are the fraction of days of each ensemble. bottom) PDFs of the Jet latitude index in February and March only, for the LIYs (solid line), the HIYs (dashed line).
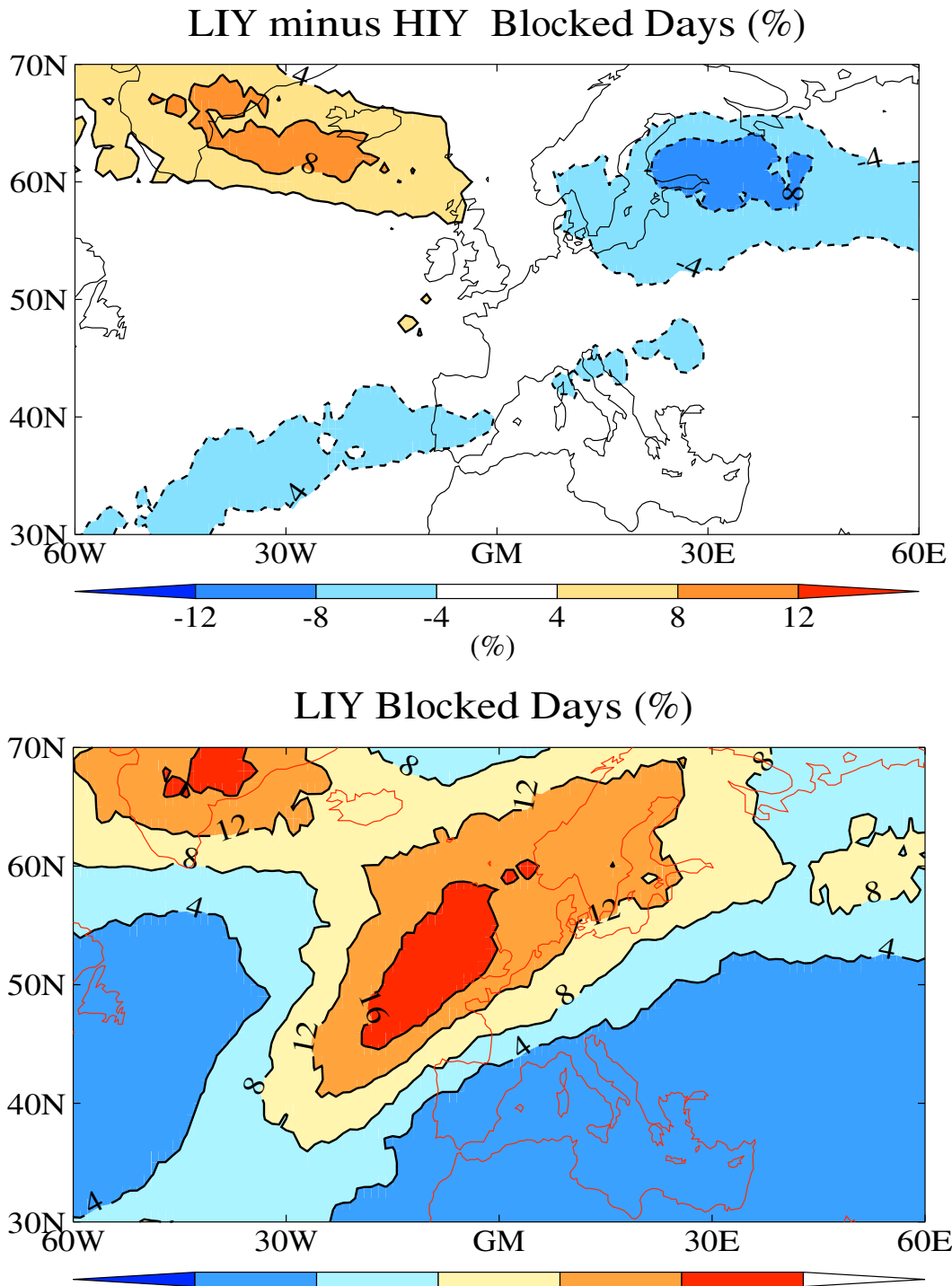
LIY minus HIY Blocked Days (%)

LIY Blocked Days (%)

Figure 8: TM90 index for LIYs (bottom) and LIYs minus HIYs (top). Values are percentage of the total days of each subset. A value of 10% corresponds to about 6 blocked days for each year (FM). The composite highlights the location of the increased high latitude blocking in the North Atlantic Sector.
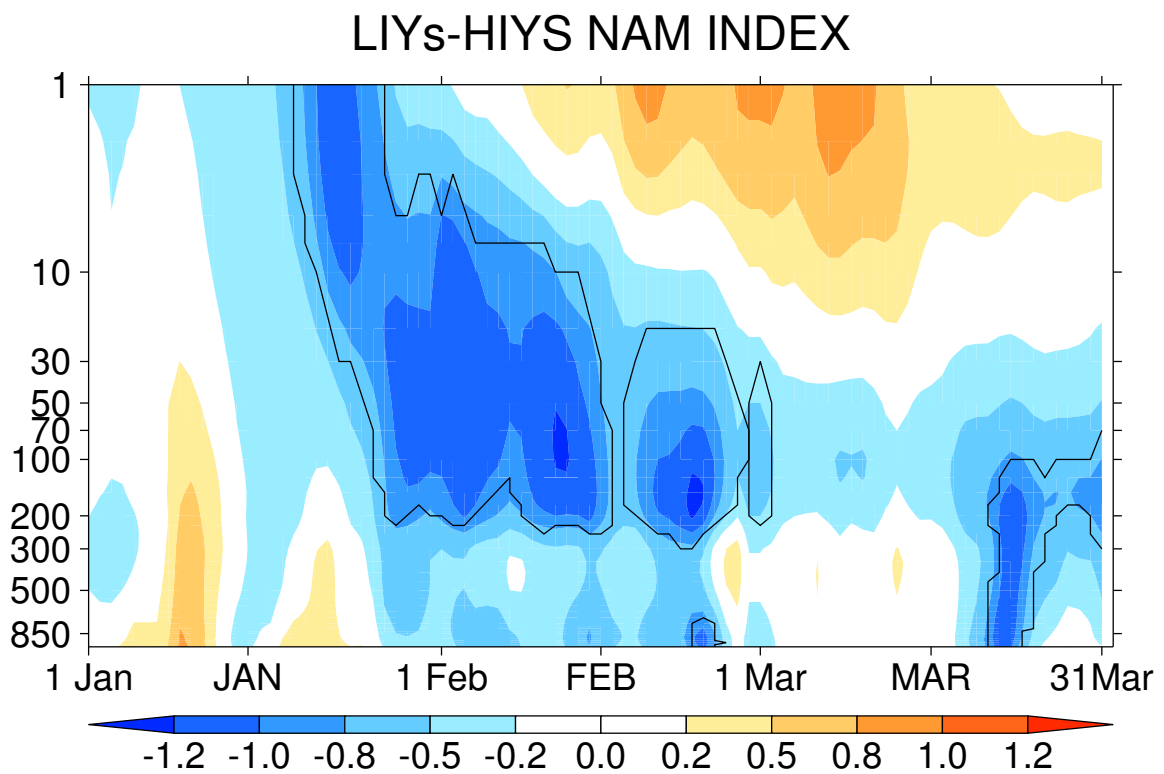
LIYs-HIYS NAM INDEX

Figure 9: *Height-Time cross section of the NAM index in JFM. Solid lines encompass statically significant values at 95% confidence level.*

Regional GPH-Index LIYs

Regional GPH-Index HIYs

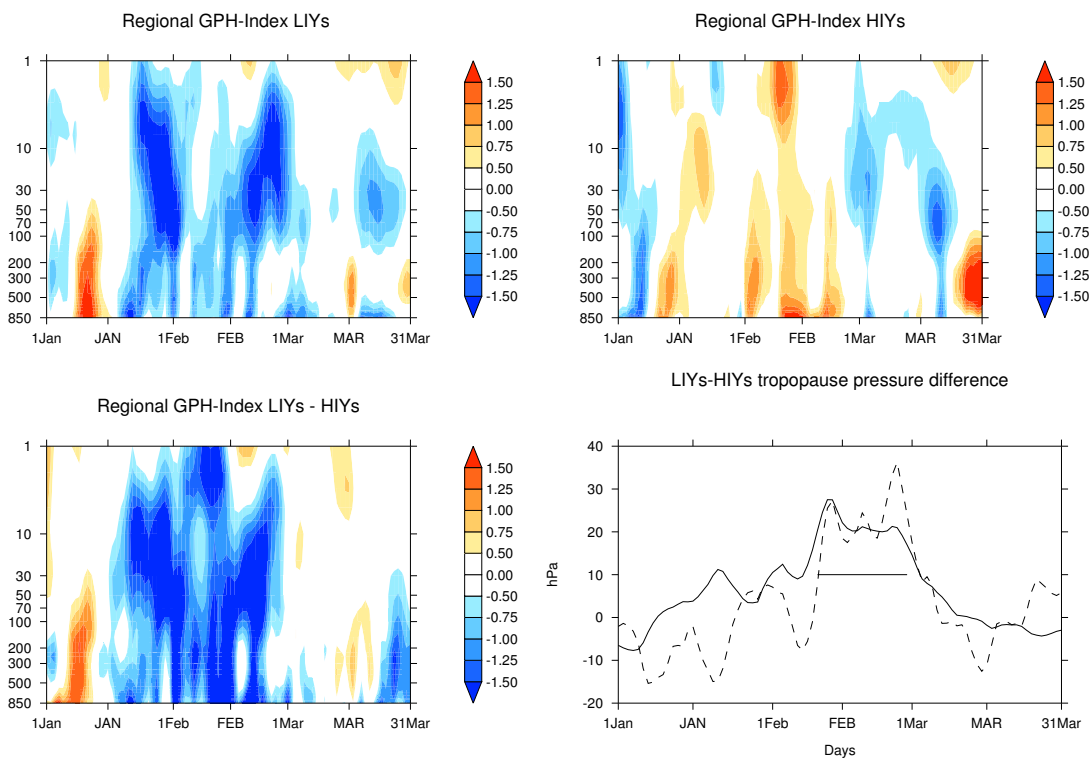Regional GPH-Index LIYs - HIYs

LIYs-HIYs tropopause pressure difference

Figure 10: a) Regional Geopotential Index for LIYs, b) HIYs and c) LIYs minus HIYs. d) Tropopause pressure difference in the polar cap (60°N- 90°N - solid line) and over Europe (0°E-40°E/45°N-55°N - dashed line).
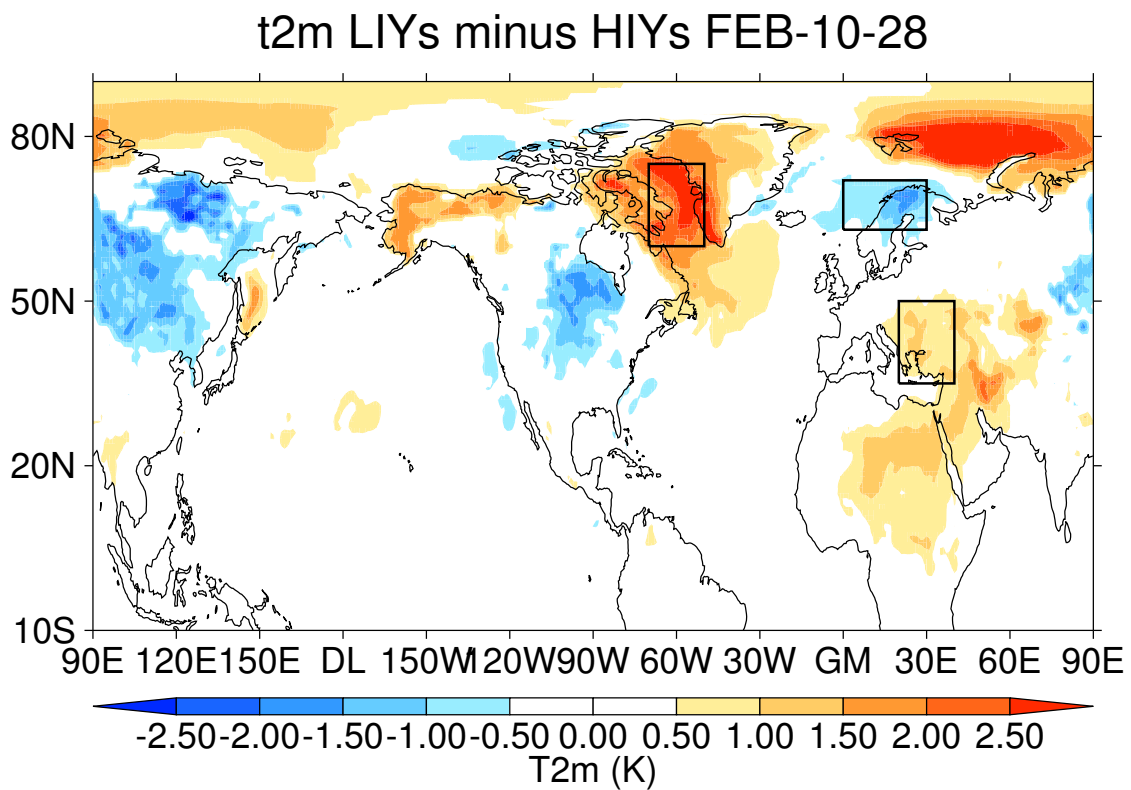
t2m LIYs minus HIYs FEB-10-28

Figure 11: Top) T2m difference (LIYs minus HIYs) for the time interval marked by the horizontal line in figure 10d. Only values exciding the 95% confidence level are plotted. Black solid lines encompass the areas used in figure 12.
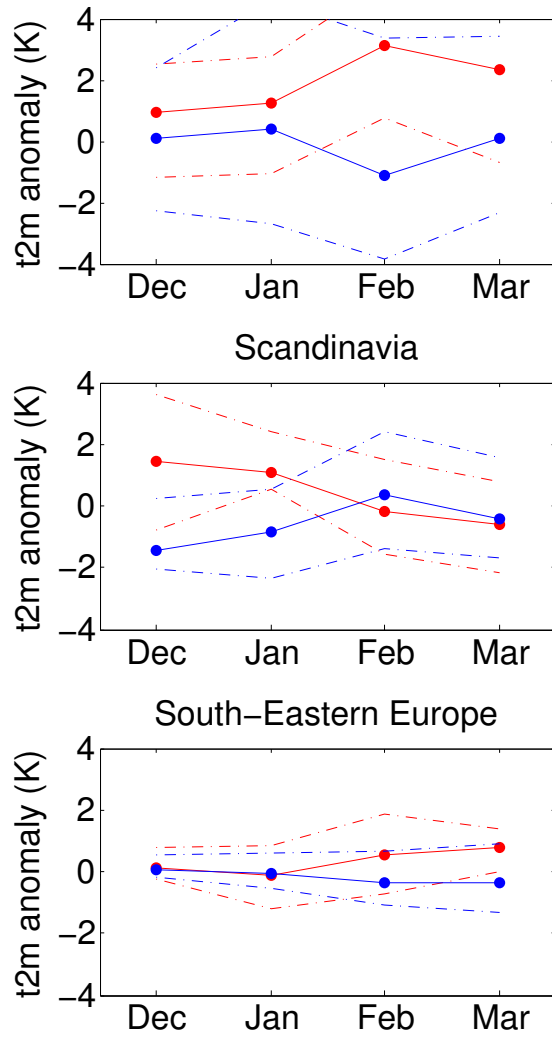
Figure 12: Time series of the monthly means of t2m anomalies for LIYs (red lines) and HIYs (blue lines) in three areas: Greenland, 70W-50W 60N-75N, b) Scandinavia 5E-35E 60N-70N, c) South-Eastern Europe, 20E-40E 30N-45N. The solid lines connect the ensemble means and the dashed lines mark the interquartile range of the distributions.
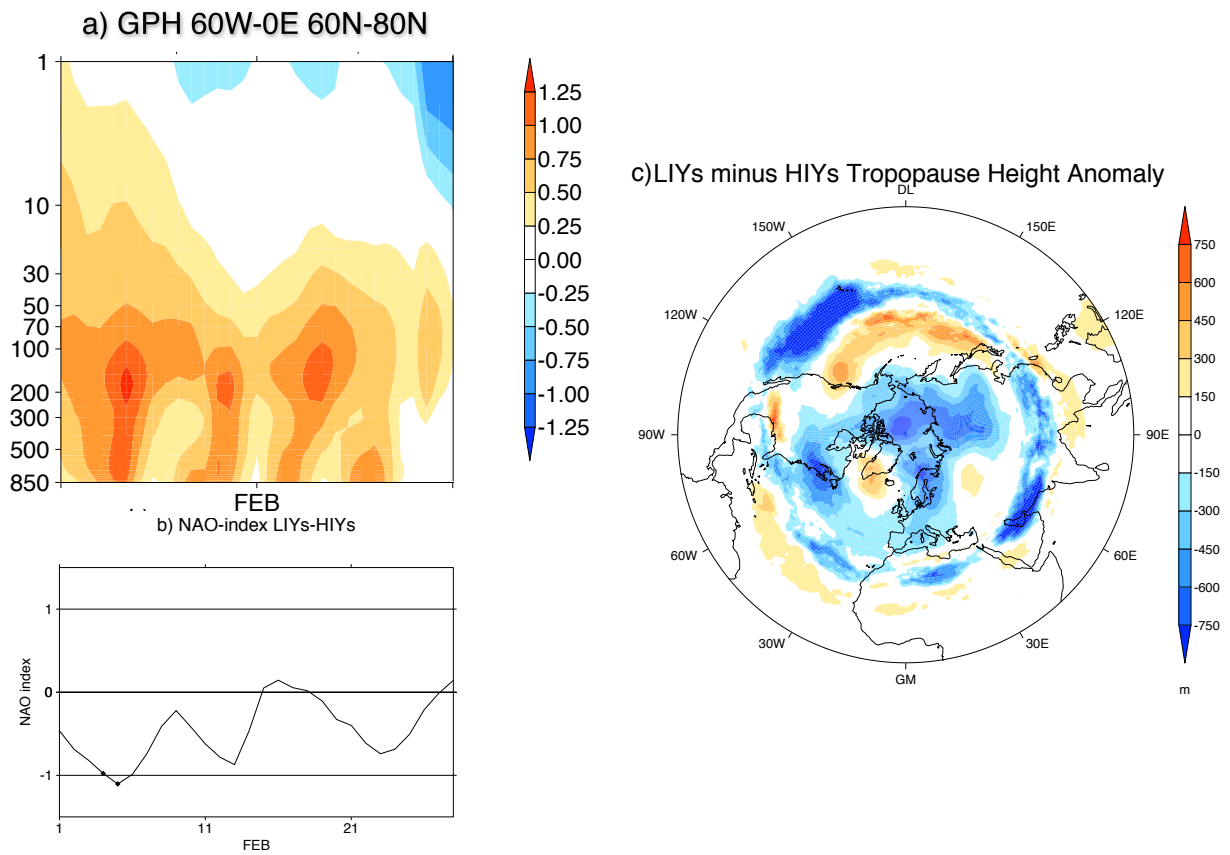
Figure 13: a) Height-Time cross section of the normalised geopotential height difference (LIYs-HIYs) in the North-Atlantic. b) Mean tropopause height difference (LIYs-HIYs) in February. c) Time series of the NAO index difference (LIYs-HIYs) in February.